Pyrazolo[3,4-*d*]pyrimidines as Potent Antiproliferative and Proapoptotic Agents toward A431 and 8701-BC Cells in Culture via Inhibition of c-Src Phosphorylation

Fabio Carraro,[†] Antonella Naldini,[†] Annalisa Pucci,[†] Giada A. Locatelli,[‡] Giovanni Maga,[‡] Silvia Schenone,*[,§] Olga Bruno,[§] Angelo Ranise,[§] Francesco Bondavalli,[§] Chiara Brullo,[§] Paola Fossa,[§] Giulia Menozzi,[§] Luisa Mosti,[§] Michele Modugno,[||] Cristina Tintori,[||] Fabrizio Manetti,[||] and Maurizio Botta[||]

Dipartimento di Fisiologia, Sezione di Neuroimmunofisiologia, Università degli Studi di Siena, Via Aldo Moro, I-53100, Siena, Italy, Istituto di Genetica Molecolare, IGM-CNR, Via Abbiategrasso 207, I-27100, Pavia, Italy, Dipartimento di Scienze Farmaceutiche, Università degli Studi di Genova, Viale Benedetto XV, I-16132, Genova, Italy, and Dipartimento Farmaco Chimico Tecnologico, Università degli Studi di Siena, Via Alcide de Gasperi 2, I-53100, Siena, Italy

Received June 24, 2005

We report here the synthesis of new pyrazolo[3,4-*d*]pyrimidine derivatives along with their biological properties as inhibitors of isolated Src and cell line proliferation (A431 and 8701-BC cells). Such compounds block the growth of cancer cells by interfering with the phosphorylation of Src, and they act as proapoptotic agents through the inhibition of the anti apoptotic gene BCL2. Several of them were found to be more active than the reference compound (1-(*tert*-butyl)-3-(4-chlorophenyl)-4-aminopyrazolo[3,4-*d*]pyrimidine, PP2) in inhibiting cell proliferation and in inducing apoptosis, and as active as PP2 in the inhibition of the phosphorylation of isolated Src. Moreover, molecular modeling simulations have been performed to hypothesize the way, at the molecular level, by which the inhibitors were able to act as antiproliferative agents.

Introduction

The understanding of the fundamental biology of cancer increased dramatically in recent years[1] and has strongly impacted on experimental and gradually also on clinical tumor therapy. We now believe that the future of tumor therapy will be represented by the development of molecularly targeted agents that specifically interfere with the key mechanisms involved in development and progression of specific types of cancer.[2] Due to their critical role in tumor development and progression, compounds able to inhibit protein kinases are of great interest in targeted cancer therapy. Protein kinases nearly control all aspects of cellular signal transmission under both physiological and pathological conditions.[1] In particular, protein-tyrosine phosphorylation catalyzed by protein tyrosine kinases (PTKs) has been implicated in the intracellular signaling cascade that acts immediately downstream of cell surface receptors to elicit a variety of cellular functions.[2] Much attention has been paid to the understanding of the structure and function of the cytoplasmic type PTKs c-Src tyrosine kinase.[3−7] The roles played by c-Src in signaling changes in the steps of cellular adhesion and motility, together with its ability to promote proliferation, are well established.[8−10] Moreover, there is experimental evidence that Src kinase is active in many tumors.[11−15] On this basis, inhibitors of the Src phosphorylation process may halt uncontrolled tumor cell growth and play an important role as new therapeutic agents for the treatment of cancer.

Although there is no approved drug acting as Src inhibitor, a plethora of compounds, potent and selective toward this kinase family, are continuously designed and synthesized. Many of them are ATP-competitive inhibitors belonging to different chemical classes. As examples, quinoline derivatives exhibit IC_{50} values up to the subnanomolar range in enzymatic assays and in the nanomolar range in Src-dependent cell proliferation assays.[16] Additional classes of important Src inhibitors are quinazoline[17] and pyrimidine derivatives. Among the latter, a huge number of pyrrolo-[18] and pyrazolo-pyrimidines[19] (such as 1-(*tert*-butyl)-3-(4-chlorophenyl)-4-aminopyrazolo[3,4-*d*]pyrimidine, PP2) have been described.

In this context, within our efforts to find new anticancer agents, we have recently reported a series of pyrazolo[3,4-*d*]-pyrimidine derivatives, found to be able to inhibit c-Src phosphorylation. Preliminary in vitro biological studies demonstrated that such compounds have a potent antiproliferative effect on the human epidermoid carcinoma A431 cells,[20] known to overexpress both EGFR and Src. This finding, together with the knowledge that the breast cancer cell line 8701-BC also overexpresses Src,[21] led us to assess the antiproliferative properties of the new compounds also toward 8701-BC cells.[22] Biological data showed that several of the reported compounds were inhibitors of 8701-BC cells[23] with noteworthy potency.

Results on both A431 and 8701-BC cells prompted us to design and synthesize additional members of the pyrazolo-pyrimidine structural class and to test them toward the same human epidermoid and human breast cancer cell lines, as well as toward isolated Src. Several of the new compounds **1**−**7** reported in this paper were found to inhibit Src phosphorylation in the micro- and sub-micromolar range, similarly to the reference compound PP2. They also selectively block cell cycle progression and promote apoptosis. Moreover, we demonstrated that the induction of apoptosis in 8701-BC cells was mediated by the inhibition of BCL2 expression. As a consequence of all these biological findings, the pyrazolo-pyrimidine derivatives disclosed here could represent a profitable tool to inhibit cancer cell growth through blocking the Src phosphorylation mechanism and inducing apoptosis.

Chemistry. Compounds **1** and **2** (Scheme 1) were prepared starting from the ethyl ester of 5-amino-1-(2-hydroxy-2-phenylethyl)-1*H*-pyrazole-4-carboxylic acid **8**, obtained following

* To whom correspondence should be addressed. Tel: 0039 010 3538866. Fax: 0039 010 3538358. E-mail: schensil@unige.it.

[†] Dipartimento di Fisiologia, Università degli Studi di Siena.

[‡] Istituto di Genetica Molecolare, IGM-CNR.

[§] Dipartimento di Scienze Farmaceutiche, Università degli Studi di Genova.

[||] Dipartimento Farmaco Chimico Tecnologico, Università degli Studi di Siena.

10.1021/jm050603r CCC: $33.50
Published on Web 02/09/2006

Scheme 1

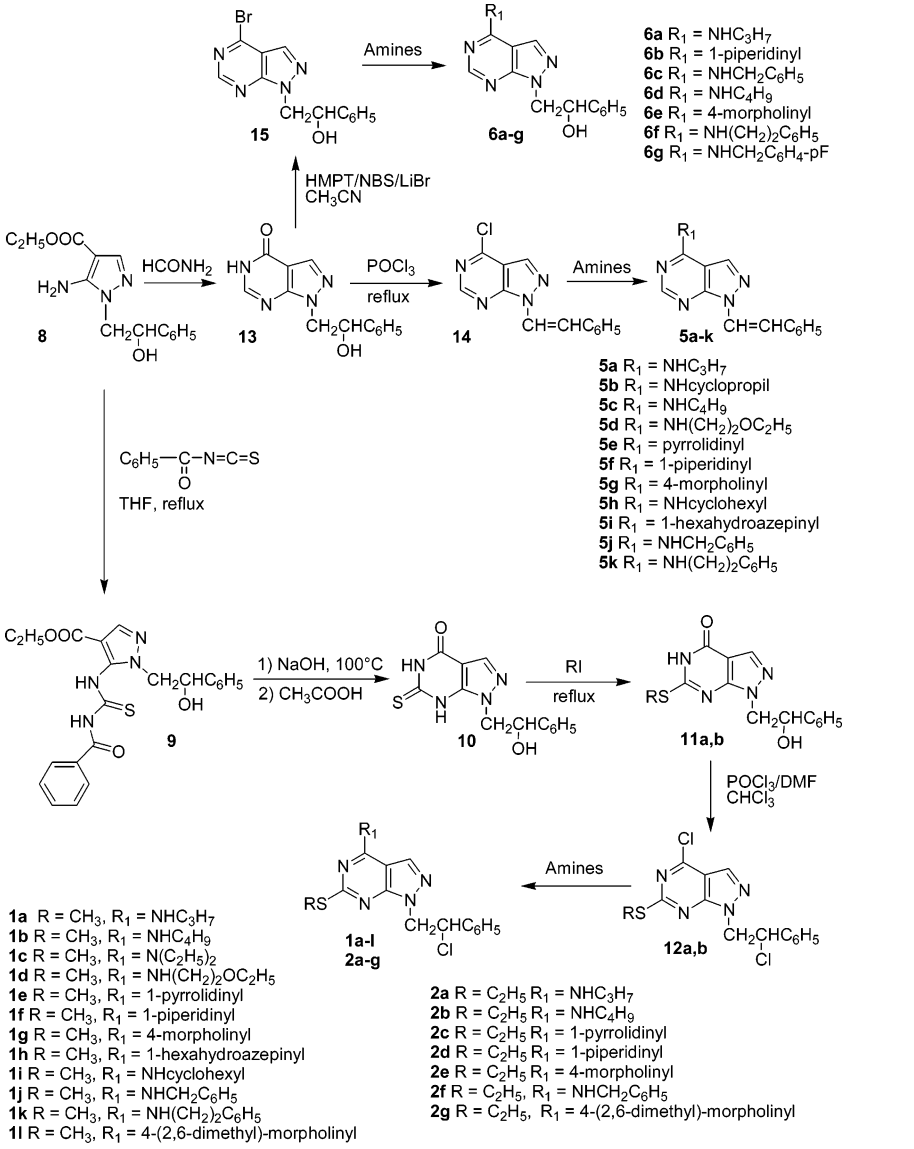

our reported procedure.[24] Reaction of **8** with benzoyl isothiocyanate in THF at reflux for 12 h yielded the intermediate **9**, which was cyclized to the pyrazolo[3,4-*d*]pyrimidine **10** by treatment with 1 M NaOH at 100 °C for 10 min, followed by acidification with acetic acid (80% yield). Alkylation of the thio group in position 6 with methyl or ethyl iodide in THF at reflux afforded the 6-thioalkyl derivatives **11**, that were in turn treated with the Vilsmeier complex ($POCl_3$:DMF, 4 equiv) in $CHCl_3$ to obtain the dihalogenated compounds **12** bearing the chlorine atom both at the position 4 of the pyrimidine nucleus and the N1 side chain. Compounds **12** were purified in good yield by chromatography on silica gel column. Finally, regioselective substitution of the C4 chlorine atom with an excess of various amines afforded the desired compounds **1** and **2** in yields ranging between 60 and 80%. Notably, the chlorine atom at the side chain has never been substituted by the amine despite its benzylic position, as shown by the ^{1}H NMR chemical shifts of the CH_2-CH side chain, which give an ABX complex pattern which it is similar to that of the starting material.

Reaction of **8** with an excess of formamide at 190 °C for 8 h afforded the pyrazolo[3,4-*d*]pyrimidinone **13** which was purified by dissolving the crude in 2 M NaOH, boiling with charcoal, followed by precipitation with acetic acid (yield 70%, mp 271−272 °C).

Reaction of **13** at reflux with $POCl_3$ afforded the 1-styryl derivative **14** which was reacted with an excess of various amines in toluene to give **5a**−**k** in good yield.

Compound **15** was prepared in a yield of 44% following the Beal and Véliz[25] procedure by treatment of **13** with a mixture of HMPT/NBS in acetonitrile at −20 °C followed by addition of LiBr and refluxing. It is interesting to point out that the secondary OH on the side chain remained unaltered by this procedure, as shown by its ^{1}H NMR spectrum. Treatment of **15** with the appropriate amines gave the desired compounds **6a**−**g**.

A number of thiomethyl derivatives **1** and thioethyl derivatives **2** were treated with an excess of DBU (1,8-diazabicyclo-[5,4,0]undec-7-ene) at 90 °C for 4 h to give the corresponding styryl derivatives **3a**−**e** and **4a**,**b** in high yield (Scheme 2). Reaction of the pyrimidinone **13** in DMF with a solution of phosphorus tribromide, pyridine and toluene at room temperature for 3 days led to the intermediate **16** (60% yield), bearing a bromine atom on the N1 side chain. Compound **16** was in turn chlorinated at C4 by treatment with the Vilsmeier complex, to afford compound **17** (80% yield) which was reacted with an excess of various amines (following the same conditions described above) to obtain derivatives **7a**−**k** in yield ranging between 60 and 80%. Also in this case the bromine atom on

Scheme 2

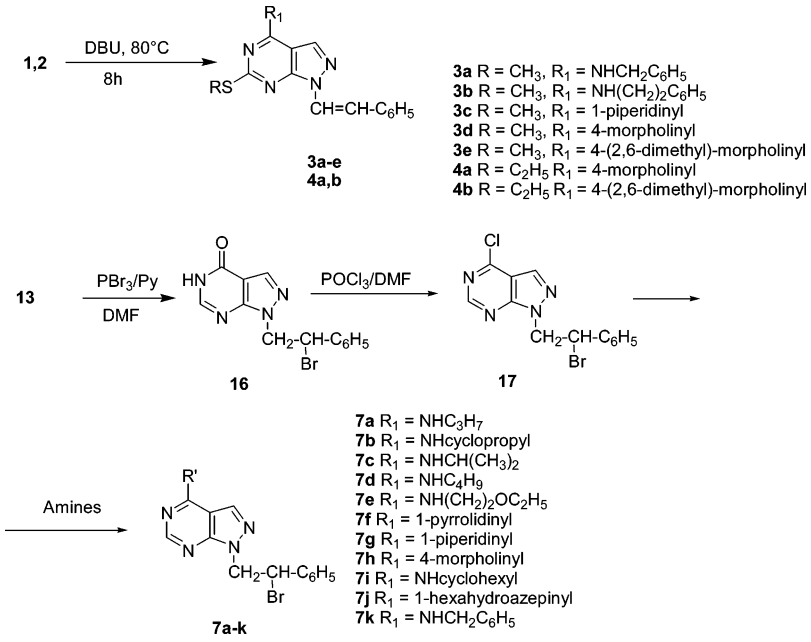

the N1 side chain was never sustituted by the amino group (Scheme 2).

Results and Discussion

Compounds **1**−**7** were evaluated for their ability to inhibit proliferation of both A431 and 8701-BC cells, as well as to interfere with Src phosphorylation. Moreover, the activity of such compounds in a cell-free assay (isolated Src) is also reported in Table 1.

To test how A431 and 8701-BC cells grown in our laboratory responded to well-known antiproliferative agents, 1-(*tert*-butyl)-3-(4-chlorophenyl)-4-aminopyrazolo[3,4-*d*]pyrimidine (PP2) was used as a reference compound, due to its potency and selectivity in inhibiting phosphorylation of the Src family tyrosine kinase members.[19,26] As a result, IC_{50} of such compound toward A431 cells (32 μM) was comparable with that reported in the literature,[19] while inhibitory activity against 8701-BC cells was about 2-fold lower (62 μM).

Cytotoxicity. The cytotoxic effect of compound was evaluated by trypan blue exclusion. Cells were stimulated for 1 h at 37 °C with increasing concentrations (10 nM to 10 μM) of the test compound in 1% FCS medium. Cells were then stained with 0.4% trypan blue in phosphate buffer saline (PBS) for 5 min. The number of dead and living cells was counted at the microscope in a blind manner. The percentage of dead cells over the total number of cells was calculated. All the compounds reported in Table 1 showed no citotoxicity (at the tested concentrations) toward both the A431 and 8701-BC cell lines.

Antiproliferative Activity. Inspection of biological data (inhibition of proliferation) suggested that compounds **1**, bearing a chlorophenylethyl side chain at N1 and a methylthio group at the position 6 on the bicyclic nucleus, were characterized by the best profile of activity toward A431 cells. In fact, nine of them (75% of compounds belonging to the subclass of compounds **1**) showed an activity comparable or higher with respect to the reference compound PP2 (32 μM). Moreover, among all the novel pyrazolo-pyrimidines presented in the paper, **1k** was the most active compound toward A431 cells.

The new compounds were also evaluated for their ability to inhibit proliferation of the breast cancer cell line 8701-BC, using the same reference compound (PP2). All compounds **1** were found to have an antiproliferative activity toward 8701-BC cells comparable or higher than that of the reference compound (62 μM), with the exception of **1c**, a 4-diethylamino derivative, showing an activity of 87 μM. Moreover, with the exception of compounds **3** and **4** (without no significant activity toward this cell line), compounds with activity higher than that of the reference compound were found among all the other subclasses. Compound **1k**, bearing a N1 phenylethyl side chain was characterized by the best biological profile, being the most active compound toward A431 cells and one of the most active compounds, together with **2a**, toward 8701-BC cells. It showed a very good activity toward the isolated Src (0.7 μM) comparable to that of PP2. Taken together, biological data showed that many of the new pyrazolo-pyrimidines showed a comparable activity toward both the cell lines, while A431 cells were more sensitive to the treatment with PP2, in comparison to the 8701-BC cell line. With the aim of better understanding the reason(s) of the antiproliferative activity of these new compounds, some of them were selected (on the basis of their biological profile in terms of activity toward both A431 and 8701-BC cells) to be submitted to further assays.

Inhibition of Src Phosphorylation. In particular, the inhibitory effect toward the phosphorylation of Src Tyr419 (a crucial step in the mechanism of the enzyme activation)[27] was first studied on cells treated with 100 nM EGF. Such a treatment is usually necessary to enhance Src phosphorylation that is generally very low. Regarding 8701-BC cells, they normally produce VEGF and EGF, and consequently Src is phosphorylated even in the 8701-BC control group (21%, Figure 1, right) (numerical values represented the percent ratio between phosphorylated and non phosphorylated Src). However, also for 8701-BC cells, an enhancement of Src phosphorylation (found to rise to 51% upon EGF treatment, Figure 1, right) is required to better appreciate the antiproliferative activity of the studied compounds.

To determine whether the new pyrazolo-pyrimidine compounds were able to inhibit the phosphorylation of Src at the level of Tyr419, we used a phosphospecific anti-Src (Tyr419) antibody (Cell Signaling Technology, Danvers, MA), with PP2 as the reference compound. Stimulation of A431 cells with EGF significantly increased phosphorylation of Src from 26% (Figure

Table 1. Structure and Physicochemical Properties of Compounds **1**−**7** and Their Antiproliferative Activity toward A431 and 8701-BC Cell Lines

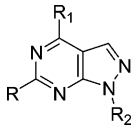

							IC$_{50}$ (μM)[c]	
compd	R	R$_1$	R$_2$[a]	mp (°C)	yield (%)	K_i (μM)[b]	8701-BC	A431
1a	SMe	NHPr	A	126−127	75	2.9 ± 0.8	64.1 ± 1.7	32.1 ± 0.5
1b	SMe	NHBu	A	106−107	45	1.7 ± 0.4	63.8 ± 2.1	27.5 ± 0.5
1c	SMe	N(Et)$_2$	A	91−92	80	0.5 ± 0.1	86.6 ± 1.2	70.2 ± 1.4
1d	SMe	NH(CH$_2$)$_2$OEt	A	115−116	68	NA	59.8 ± 3.1	31.6 ± 0.6
1e	SMe	1-pyrrolidinyl	A	151−152	53	ND	56.4 ± 1.0	32.3 ± 0.8
1f	SMe	1-piperidinyl	A	94−95	60	2.4 ± 0.7	67.5 ± 1.2	38.4 ± 0.8
1g	SMe	4-morpholinyl	A	116−117	75	6.5 ± 1.0	64.2 ± 1.8	24.3 ± 0.4
1h	SMe	1-hexahydroazepinyl	A	99−100	60	ND	54.4 ± 0.9	62.0 ± 1.2
1i	SMe	NHcyclohexyl	A	138−139	72	ND	35.5 ± 1.5	29.8 ± 1.4
1j	SMe	NHBn	A	142−143	81	3.7 ± 0.9	53.2 ± 1.2	24.8 ± 0.7
1k	SMe	NH(CH$_2$)$_2$Ph	A	73−74	76	0.7 ± 0.2	31.2 ± 0.5	18.2 ± 0.9
1l	SMe	4-(2,6-dimethyl)-morpholinyl	A	164−165	65	NA	69.9 ± 6.7	27.6 ± 1.0
2a	SEt	NHPr	A	74−75	75	0.7 ± 0.1	29.5 ± 0.9	79.1 ± 1.8
2b	SEt	NHBu	A	100−101	45	0.6 ± 0.2	38.8 ± 0.5	40.4 ± 0.4
2c	SEt	1-pyrrolidinyl	A	131−132	65	ND	71.7 ± 1.9	88.9 ± 1.7
2d	SEt	1-piperidinyl	A	99−100	65	8.6 ± 1.3	NA	NA
2e	SEt	4-morpholinyl	A	130−131	80	3.6 ± 0.9	79.8 ± 3.0	42.3 ± 0.7
2f	SEt	NHBn	A	165−166	85	8.2 ± 1.4	43.3 ± 1.2	NA
2g	SEt	4-(2,6-dimethyl)-morpholinyl	A	112−113	72	NA	96.5 ± 4.1	50.7 ± 1.3
3a	SMe	NHBn	B	185−186	70	NA	82.4 ± 2.3	39.9 ± 0.6
3b	SMe	NH(CH$_2$)$_2$Ph	B	121−122	65	NA	95.1 ± 1.9	53.9 ± 1.7
3c	SMe	1-piperidinyl	B	155−156	67	NA	NA	49.8 ± 0.7
3d	SMe	4-morpholinyl	B	161−162	75	NA	81.7 ± 2.4	35.7 ± 0.6
3e	SMe	4-(2,6-dimethyl)-morpholinyl	B	160−161	65	NA	94.2 ± 1.4	74.4 ± 2.8
4a	SEt	4-morpholinyl	B	155−156	75	NA	87.2 ± 2.5	49.8 ± 0.8
4b	SEt	4-(2,6-dimethyl)-morpholinyl	B	147−148	65	23 ± 6	NA	42.0 ± 1.0
5a	H	NHPr	B	189−190	86	ND	56.8 ± 2.4	61.3 ± 1.0
5b	H	NHcyclopropyl	B	220−221	74	9.2 ± 1.4	68.0 ± 1.8	81.1 ± 2.2
5c	H	NHBu	B	145−146	64	NA	80.5 ± 6.8	91.4 ± 2.0
5d	H	NH(CH$_2$)$_2$OEt	B	115−116	84	ND	43.1 ± 1.3	49.4 ± 2.7
5e	H	1-pyrrolidinyl	B	159−160	95	NA	50.5 ± 0.7	62.7 ± 1.0
5f	H	1-piperidinyl	B	157−158	80	NA	NA	69.1 ± 1.2
5 g	H	4-morpholinyl	B	172−173	85	NA	58.8 ± 0.7	59.1 ± 1.0
5h	H	NHcyclohexyl	B	187−188	80	12 ± 2.5	49.8 ± 0.7	NA
5i	H	hexahydroazepinyl	B	190−191	72	NA	93.7 ± 0.6	60.9 ± 2.1
5j	H	NHBn	B	184−185	81	2.4 ± 0.4	65.1 ± 1.2	NA
5k	H	NH(CH$_2$)$_2$Ph	B	152−153	78	NA	65.1 ± 2.1	NA
6a	H	NHPr	C	172−173	74	NA	NA	91.2 ± 1.4
6b	H	1-piperidinyl	C	168−169	68	NA	NA	86.4 ± 1.6
6c	H	NHBn	C	169−170	58	2.4 ± 0.6	NA	81.7 ± 3.2
6d	H	NHBu	C	125−126	80	NA	NA	82.9 ± 1.8
6e	H	4-morpholinyl	C	179−180	75	NA	NA	84.2 ± 3.7
6f	H	NH(CH$_2$)$_2$Ph	C	132−133	77	2.4 ± 0.9	45.8 ± 1.5	77.1 ± 2.9
6 g	H	NHCH$_2$C$_6$H$_4$-*p*-F	C	149−150	62	NA	64.5 ± 5.1	91.7 ± 2.4
7a	H	NHPr	D	136−137	60	0.9 ± 0.2	NA	60.5 ± 2.7
7b	H	NHcyclopropyl	D	162−163	70	ND	89.0 ± 1.7	49.6 ± 2.4
7c	H	NH*i*Pr	D	150−151	65	2.8 ± 0.8	78.6 ± 1.5	45.9 ± 2.1
7d	H	NHBu	D	95−96	70	2.9 ± 1.0	37.4 ± 0.9	33.6 ± 2.0
7e	H	NH(CH$_2$)$_2$OEt	D	109−110	60	2.7 ± 0.5	89.8 ± 3.2	40.1 ± 2.1
7f	H	1-pyrrolidinyl	D	127−128	65	9.6 ± 2.2	NA	78.8 ± 3.2
7 g	H	1-piperidinyl	D	144−145	68	1.6 ± 0.5	NA	35.1 ± 0.7
7h	H	4-morpholinyl	D	111−112	67	ND	NA	19.2 ± 0.9
7i	H	NHcyclohexyl	D	154−155	70	ND	NA	28.2 ± 1.9
7j	H	1-hexahydroazepinyl	D	124−125	64	ND	63.8 ± 1.8	57.6 ± 3.1
7k	H	NHBn	D	157−158	80	3.3 ± 0.5	43.5 ± 0.8	41.7 ± 1.7
PP2[d]						0.5 ± 0.1	61.8 ± 4.4	32.2 ± 0.7

[a] A = 2-chloro-2-phenylethyl, B = styryl, C = 2-hydroxy-2-phenylethyl, D = 2-bromo-2-phenylethyl. [b] Calculated from eq 2, where E_0 = 0.0125 μM and S_0 = 0.0160 μM. NA = Not active (ID$_{50}$ > 2 mM). ND = Not determined. [c] IC$_{50}$ values are means ± SEM of series separate assays, each performed in quadruplicate. NA = not active at 100 μM. [d] Since PP2 is a noncompetitive inhibitor, ID$_{50}$ = K_i.

2, control) to 55% (Figure 2, control + EGF). PP2 strongly inhibited the stimulated cells (21% phospho/non phospho), similarly to that found for **2b**, **5a**, and **5i**. Interestingly, compounds **1f**, **1j**, and **1k** showed an inhibitory activity (8% ratio) more pronounced with respect to PP2. Finally, **1g** and **2e** were characterized by a slight, nonsignificant reduction of Src phosphorylation, even if they showed high antiproliferative activity (24 μM, better than PP2, and 42 μM, respectively).

Similar experiments were performed to evaluate the inhibitory properties of compounds **1f**, **1j**, **1k**, **2b**, **2e**, and **6e** toward the phosphorylation of Src on the 8701-BC cell line (Figure 1). As previously found for A431 cells, EGF stimulation induced a

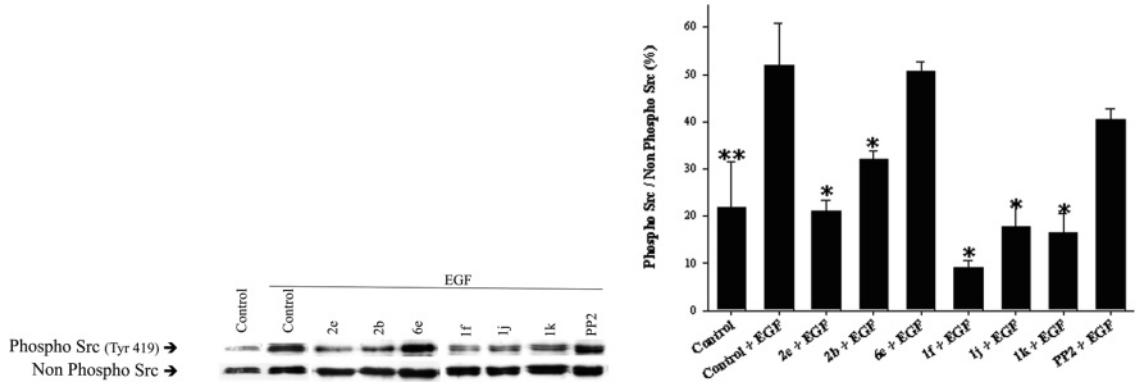

Figure 1. Effect of compounds **1f**, **1j**, **1k**, **2b**, **2e**, and **6e** on the phosphorylation of Src in 8701-BC cells, in comparison to PP2 (reference compound). 8701-BC cells were cultured at a concentration of 2×10^4 cells/mL. (left) Lane 1: cell control; lane 2: cells treated for 5 min with EGF (100 nM); lane 3−8: cells challenged for 3 h in the presence of 10 μM of the tested compound and then treated for 5 min with EGF (100 nM); lane 9 cells challenged for 3 h in the presence of 10 μM of PP2 and then treated for 5 min with EGF (100 nM). After 3 h, cell lysates were obtained and analyzed. Immunoblot analysis was performed using phospho-specific antibodies to Src (Tyr419). Filters were additionally reprobed with specific non phospho anti-Src antibodies after stripping. Results are representative of three independent experiments. (right) Quantification of phospho and non phospho Src expression was achieved with Sigma Gel analysis software and the results represented the percent of the phospho Scr over non phospho Src. The means ± SEM of three independent experiments are presented. A double asterisk (**) indicates a significant ($p < 0.05$) effect of EGF treatment (control vs control + EGF). Single asterisks (*) indicate statistically significant differences between control + EGF and 8701-BC cells treated with specific compound + EGF. The statistical analyses were performed using Student's *t* test and the Bonferroni's correction.

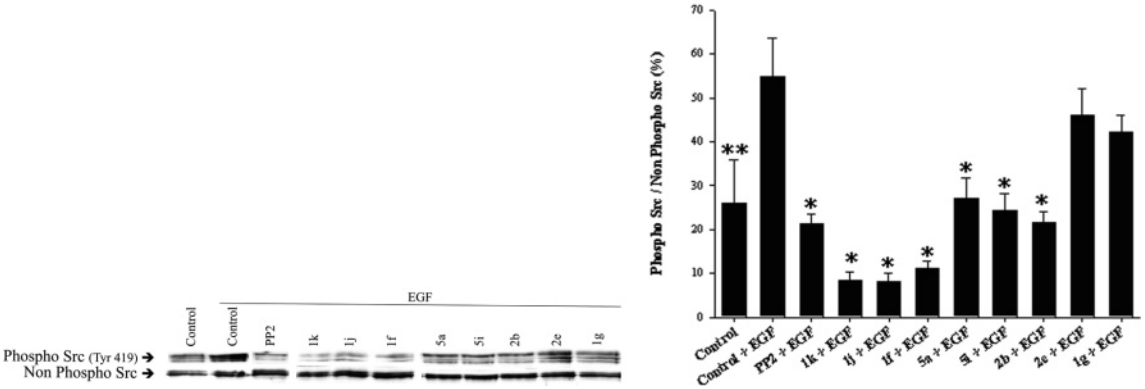

Figure 2. Effect of compounds **1f**, **1g**, **1j**, **1k**, **2b**, **2e**, **5a**, and **5i** on the phosphorylation of Src in A431 cells, in comparison to PP2 (reference compound). A431 were cultured at a concentration of 2×10^4 cells/mL. (left) Lane 1: cell control; lane 2: cells treated for 5 min with EGF (100 nM); lane 3: cells challenged for 3 h in the presence of 10 μM PP2 and then treated for 5 min with EGF (100 nM); lane 4−11: cells challenged for 3 h in the presence of 10 μM of the tested compound and then treated for 5 min with EGF (100 nM). After 3 h, cell lysates were obtained and analyzed. Immunoblot analysis was performed using phospho-specific antibodies to Src (Tyr419). Filters were additionally reprobed with specific non phospho anti-Src antibodies after stripping. Results are representative of three independent experiments. (right) Quantification of phospho and non phospho Src expression was achieved with Sigma Gel analysis software, and results represented the percent of the phospho Scr over non phospho Src. The means ± SEM of three independent experiments are presented. A double asterisk (**) indicates a significant ($p < 0.05$) effect of EGF treatment (control vs control + EGF). Single asterisks indicate statistically significant differences between control + EGF and A431 cells treated with specific compound + EGF. Statistical analyses were performed using Student's *t* test and the Bonferroni's correction.

marked increase of Src phosphorylation. On the other hand, PP2 showed a reduced ability to inhibit phosphorylation (about 40% ratio), while all the compounds tested, with the exception of **6e**, were characterized by inhibitory properties better than that of the reference compound. Similarly to that found for A341 cells, compounds **1f**, **1j**, and **1k** showed high inhibition of phosphorylation with a phospho/non phospho ratio lower than 20%.

Studies on Isolated Src. The mechanism of cell growth inhibition was further investigated in a cell-free assay and it was found to be competitive with the ATP substrate but not with a peptide used as a Src substrate.[28] Several of the compounds tested showed inhibitory activity toward the isolate Src in the micro- and sub-micromolar range. It is worth mentioning that some of them showed an activity in cellular assays higher than that in the in vitro inhibition assay (Table 1). There are, at least, two possible explanations. A first one relates to the artificial conditions of the enzymatic assay. In fact, it is well-known that in vivo the activity of Src is modulated by its cellular context, as well as by the different substrates.[29] Upon binding to a substrate, Src is subjected to extensive conformational changes. Moreover, the presence of specific phosphorylated residues in the substrate plays an important role in attracting Src and stabilizing its binding. In our in vitro system, we used an artificial substrate, namely a short peptide. It is possible, then, that the catalytic efficiency, as well as the conformation of the enzyme, were suboptimal under our in vitro conditions, with respect to the physiological context of an intact cell. This is likely reflected by the rather low affinity ($K_m = 30$ μM) displayed by the recombinant enzyme for the peptidic substrate and could influence also the affinity of the enzyme for our inhibitors. Indeed, the activity of the reference compound PP2 was found to be 0.5 μM, whereas data in the literature report a lower activity. Another possible explanation for the higher activities detected in cell-based assays is the possibility that our compounds target also other kinases. In fact, preliminary

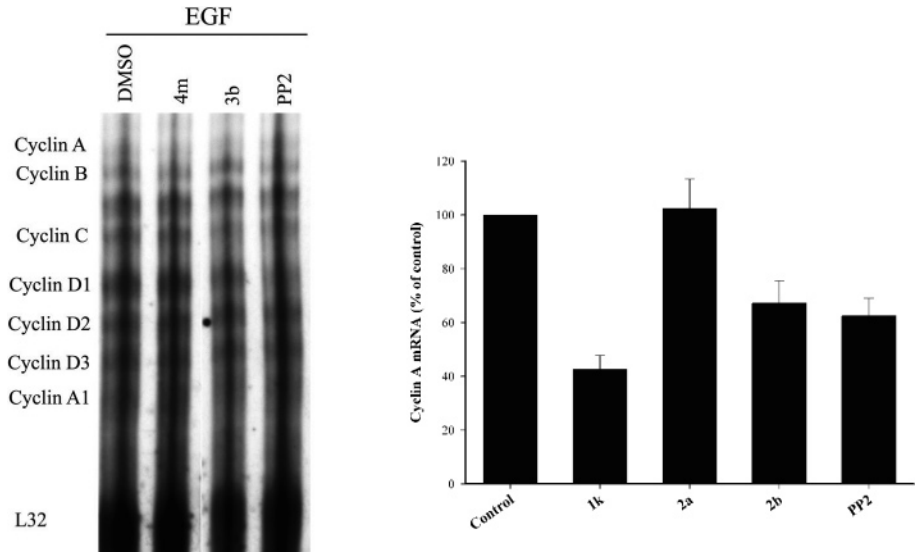

Figure 3. Cyclin A inhibition. 8701-BC cells were cultured at a concentration of 2×10^4 cells/mL in the absence and in the presence of 10 μM of the tested compound for 3 h at 37 °C, in comparison to PP2 used as the reference compound. Cell lysates from control and treated 8701-BC cells were obtained and analyzed by RNAse protection assay. L32 was used as a housekeeping gene. Quantification of cyclin A expression was achieved with Sigma Gel analysis software, and the results, representing the percentage of inhibition over control, are presented (right).

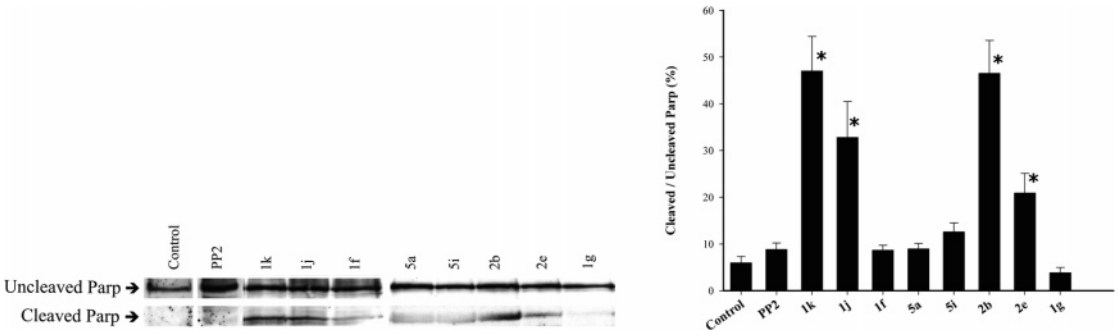

Figure 4. Proapoptotic effect of compounds **1f**, **1g**, **1j**, **1k**, **2b**, **2e**, **5a**, and **5i** measured by PARP cleavage, in comparison to PP2 (reference compound). A431 cells were cultured at a concentration of 2×10^4 cells/mL. (left) Lane 1: cell control; lane 2: cells challenged for 3 h with 10 μM PP2; lane 3−10: cells challenged for 3 h in the presence of 10 μM of the tested compound. After 3 h, cell lysates were obtained and analyzed. Immunoblot analysis was performed using PARP-specific antibodies to both the uncleaved (113 kDa) and cleaved (89 kDa) form of parp. (right) Quantification of PARP expression was achieved with Sigma Gel analysis software, and the results, representing the percent of cleaved over uncleaved PARP, are expressed as means ± SEM of three independent experiments. Asterisks indicate statistically significant differences ($p < 0.05$) between control and A431 cells treated with the tested compound. Statistical analyses were performed using Student's *t* test and the Bonferroni's correction.

experiments showed that several of the new compounds were active also against other nonreceptor, or cytoplasmic, tyrosine kinases and demonstrate activity toward malignant cells expressing c-kit.[30] Nevertheless, we are still unable to rule out if such compounds, in addition to be competitive for ATP, could or not act through a mixed-mode of Src inhibition or interact with an allosteric site on Src.[31]

Studies on Cyclins. We were also interested in investigating wether the inhibition of c-Src could result in an alteration of the cyclins. Cell cycle progression through the G1 phase is regulated by the cyclin dependent kinase (CDK) 4 and CDK2 activities under the control of cyclins D (namely, D1, D2 and D3) and E, while cyclins A and B are considered important mitotic agents and their expression is necessary for cells to enter S phase and progress from G2 into mitosis.[32] Using the ribonuclease protection assay (RPA) technique, we demonstrated that the inhibition of Src was sufficient to reduce the cyclin mRNA expression on 8701-BC cell line. In particular, compounds **1k**, **2b**, and PP2 were able to reduce cyclin A expression (Figure 3).

Proapoptotic Activity. Prompted by the ability of such compounds in reducing Src phosphorylation of both A431 and 8701-BC cell lines, we also tested their proapoptotic activity on a Poly-ADP−Ribose-Polymerase (PARP) assay (Figures 4 and 5). PARP is a 113 kDa zinc-dependent protein that binds specifically at DNA strand breaks produced by various genotoxic agents.[33] PARP is also a substrate for certain caspases (e.g. caspase 3 and 7) activated during early stages of apoptosis. These proteases cleave PARP to fragments of approximately 89 and 24 kDa. Thus, detection of the 89 kDa PARP fragment with specific anti-PARP antibodies represents an early marker for apoptosis.[34] Figure 4 shows that compounds **1k** and **2b** potently induced apoptosis in A431 cells (48% of cleaved/uncleaved PARP ratio), while **1j** and **2e** showed lower, but significant, proapoptotic activity (32 and 21% ratio, respectively). All the remaining compounds, including PP2, were characterized by an unsignificant proapoptotic activity, comparable to that found in the control (6 to 12% ratio). As for 8701-BC cells is concerned, the cleaved/uncleaved PARP ratio of the control was about 23% (Figure 5), while proapoptotic activity of all the tested inhibitors was comparable each other. In fact, while **2b** was the most interesting compound (43%), the proapoptotic activity of the remaining compounds was found to be in the range between 28% (**1j**) and 38% (PP2).

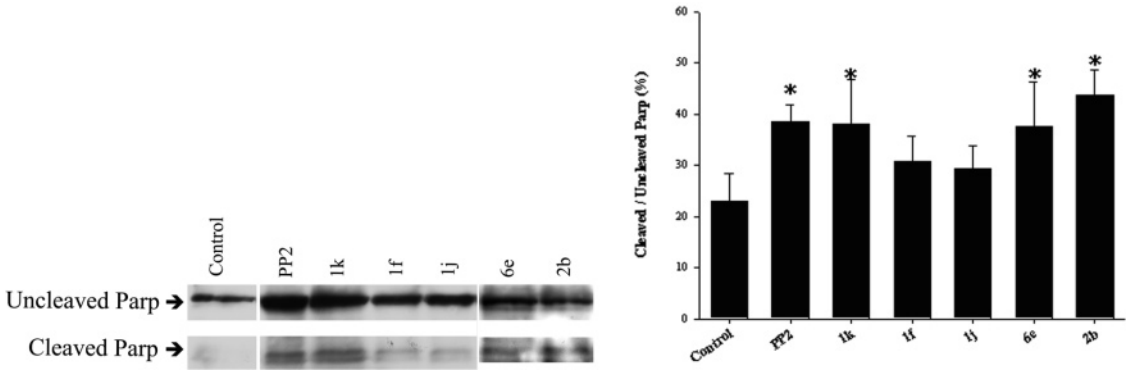

Figure 5. Proapoptotic effect of the compounds **1f**, **1j**, **1k**, **2b**, and **6e** measured by PARP cleavage in 8701-BC cells, in comparison to PP2 (reference compound). 8701-BC cells were cultured at a concentration of 2×10^4 cells/mL. (left) Lane 1: cell control; lane 2: cells challenged for 3 h with 10 μM of PP2; lane 3−7: cells challenged for 3 h in the presence of 10 μM of the tested compound. After 3 h, cell lysates were obtained and analyzed. Immunoblot analysis was performed using PARP-specific antibodies to both the uncleaved (113 kDa) and cleaved (89 kDa) form of parp. (right) Quantification of PARP expression was achieved with Sigma Gel analysis software and the results, representing the percent of cleaved over uncleaved PARP, are expressed as means ± SEM of three independent experiments. Asterisks indicate statistically significant differences ($p < 0.05$) between control and 8701-BC cells treated with specific compound. The statistical analyses were performed using Student's *t* test and the Bonferroni's correction.

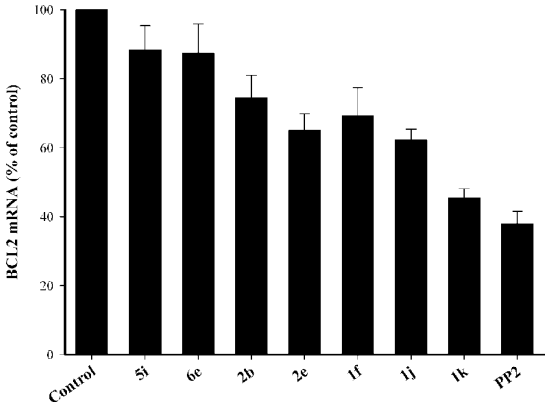

Figure 6. Inhibition of the anti apoptotic gene BCL2. 8701-BC cells were cultured at a concentration of 2×10^4 cells/mL in the absence and in the presence of 10 μM of the tested compound for 3 h at 37 °C, in comparison to PP2, used as the reference compound. Cell lysates from control and treated 8701-BC cells were obtained and analyzed by RNAse protection assay. L32 was used as a housekeeping gene. Quantification of BCL2 expression was achieved with Sigma Gel analysis software and the results, representing the percentage of inhibition over control, are presented.

Studies on BCL2. Finally, on the basis of the ability of some of these compounds to induce apoptosis in both cell lines, we also investigated the expression of BCL2 mRNA by RPA. BCL2 is an integral membrane 26 kDa protein which, when overexpressed, especially in tumor cell lines, blocks apoptosis.[35] The inhibition of the anti apoptotic gene BCL2 (Figure 6) could help in explaining the molecular mechanism of apoptosis induction.

Molecular Docking Simulations. Molecular modeling simulations have been performed to hypothesize the way by which the inhibitors bind Src and to gain insight on the peculiar chemical features that influenced their activity toward the isolated enzyme. In detail, the new pyrazolo-pyrimidines were found to inhibit Src phosphorylation on both A431 and 8701-BC cell lines, as well as to be ATP-competitive inhibitors in a cell-free assay (isolated Src). Based on this experimental evidence, molecular docking simulations followed by optimization of the resulting complexes between Src and its inhibitors have been performed. To this aim, the reliability of the docking protocol was first checked by simulation of the interactions between PP2 and Src and comparison of the modeled complexes with the experimental and theoretical data already available. In detail, in the first step, the three-dimensional structure of c-Src in an active conformation (entry 1Y57 of the Brookhaven Protein Data Bank)[36] was relaxed through an energy minimization routine (all-atom Amber* force field, Polack−Ribiere conjugate gradient method, continuum solvation with water, extended cutoffs, convergence at 0.01 kJ/mol·Å) to avoid any steric bump eventually occurred in the X-ray structure. Next, the software Autodock3.0[37] was chosen as the tool to perform docking simulations of PP2 onto the Src structure. As a result, within the first and most populated cluster of orientations/conformations ranked by the software, PP2 showed an orientation with the network of hydrogen bond contacts (involving Met341 and Glu339) and hydrophobic interactions reported in a theoretical model previously published,[38] and also in agreement with the binding orientation and interactions of PP2 onto the Lck structure[39] (the template structure usually used to model by homology the structure of Src in its active form). Taken together, these results led us to hypothesize that the computational approach can be considered as a reliable modeling procedure to be applied for finding the orientations and interactions of ligands inside the kinase domain of Src. In addition, to further assess the reliability of Autodock results, we have performed additional simulations by means of the software MacroModel.[40] In detail, we have applied a docking protocol that allows for rotation and translation of the inhibitor within the kinase domain of Src. Moreover, all the rotatable bonds of the inhibitor were submitted to a statistical conformational search according to a procedure previously reported.[41] As a result, the best conformational model was very similar to the first orientation found by Autodock, with slight differences in the orientation of both N1 and C4 side chains (the root-mean-square deviation calculated on all the heavy atoms was found to be 0.32 Å).

Once the reliability of the docking procedure was tested, the interaction pathway between inhibitors and Src was simulated applying the same protocol used for PP2. Simulations allowed for the identification of two different binding modes, depending on the presence or on the absence of an alkylthio substituent at position 6 of the pyrazolo-pyrimidine ring.

In general, compounds unsubstituted at position 6 showed an interaction pathway similar to that of PP2 (Figure 7). In particular, both N5 and the amino group at C4 are involved in two hydrogen bonds with the NH and the carbonyl backbone groups of Met341, respectively, similarly to that found for PP2

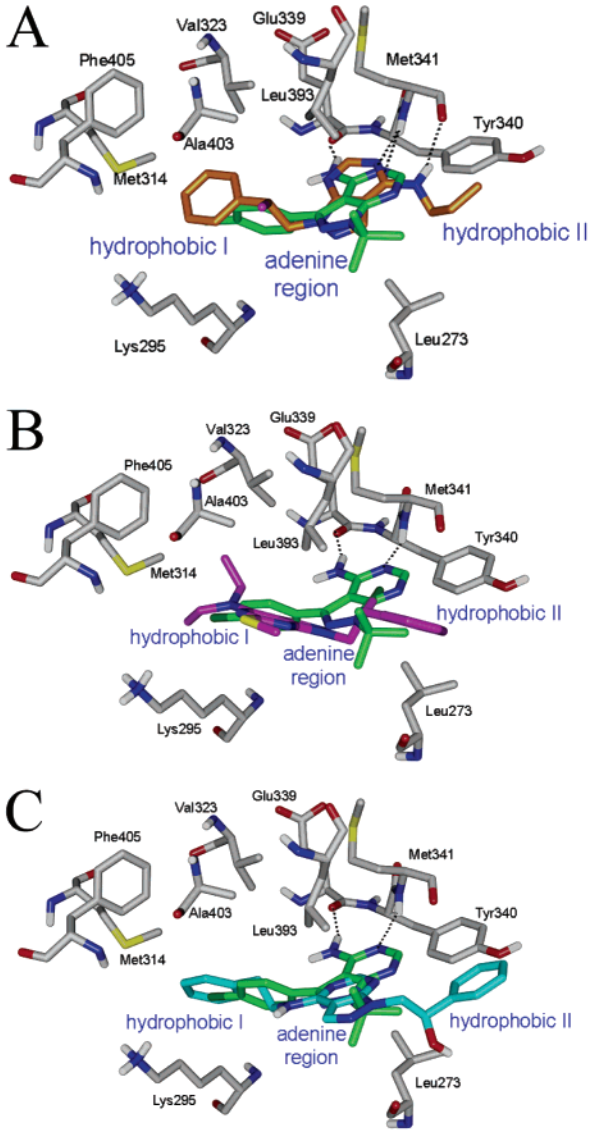

Figure 7. Graphical representation of the binding mode of the new compounds into the ATP binding site of the active form of Src, in comparison to the orientation of PP2 (green). For sake of clarity, only a few residues are displayed, nonpolar hydrogen atoms are omitted, and hydrogen bond interactions are represented by black dashed lines. (A) The best conformer of **7a** (orange) is able to make a network of hydrogen bonds with the receptor counterpart, similar to that of PP2. (B) Compound **1c** (magenta) in its best orientation lacks the network of hydrogen bond with amino acid residues. (C) The orientation of **6f** (cyan) into the Src binding site is the same found for all compounds bearing a phenylethylamino side chain at C4.

that interacted with Met341 and Glu339. Moreover, the N1 side chain of the new compounds, superposed to the *p*-chlorophenyl group of PP2, was located into the hydrophobic pocket I, interacting with Thr338, Lys295, Val281, Met314, Val323, Ala293, and Phe405. On the other hand, substituents at C4, similarly to the *tert*-butyl moiety of PP2, are accommodated within the hydrophobic pocket II, showing favorable lipophilic contacts with Gly344, Tyr340, and Leu273. Finally, the heterocyclic cores shared a common location within the adenine region of the ATP binding site.

In the alternative binding mode, compounds bearing an alkylthio substituent at position 6, although located within the kinase domain, showed a different orientation with respect to 6-unsubstituted compounds described above and PP2 (Figure 7). In particular, the alkylthio substituent seemed to be responsible for a reorientation of the heterocyclic nucleus that approached the hydrophobic region I, also occupied by C4 substituents. On the other hand, N1 substituents were partially inserted into the adenine region and directed toward the hydrophobic pocket II. Methyl- or ethylthio groups were located into an additional hydrophobic region and were involved in favorable interactions with Leu393 and Ala403. Differently from PP2 and 6-unsubstituted compounds, the structure of 6-alkylthio derivatives was not engaged in any hydrogen bond. Interestingly, the lack of the hydrogen bond network was in general not associated with inactivity, as shown in Table 1. In fact, despite the different orientation and the absence of any hydrogen bond, several compounds bearing an alkylthio substituent at position 6 were endowed with an inhibitory activity comparable to C6 unsubstituted compounds. As an example, **1c** was the most active compound of the whole set. Thus, docking studies suggested that hydrogen bond contacts were not essential for the activity of 6-alkylthio pyrazolo-pyrimidine derivatives. These findings were also in agreement with the fact that several 6-unsubstituted compounds, unable to establish a hydrogen bond donor−acceptor network due to the lack of a NH group at C4 (i.e., **7f** and **7g**), maintained a good inhibitory activity. Alternatively, one might suppose that 6-alkylthio derivatives counterbalanced the loss of hydrogen bond interactions with additional hydrophobic interactions involving the alkylthio side chains. In this context, computational studies showed that lipophilic interactions resulting from full occupancy of hydrophobic regions I and II seemed to play a crucial role for the activity of ligands. On this basis, the lack of activity that affected most compounds with a hydroxy side chain at N1 could be accounted by the unsatisfactory filling of the hydrophobic pocket I, due to the presence of a hydrophilic hydroxy group on the N1 side chain.

Finally, it is worth noting that compounds with a phenylethylamino substituent at position 4 showed a peculiar behavior, being located with a common orientation, independent from the presence of an alkylthio substituent at position 6 (Figure 7). In fact, such compounds disposed their pyrazolo-pyrimidine nucleus in the adenine region, the phenylethylamino moiety in the hydrophobic region I, and the C4 side chain in the hydrophobic region II. The alkylthio substituent, when present, lay in the adenine region, without altering the orientation of the heterocyclic ring.

Conclusions

The synthesis of a series of pyrazolo[3,4-*d*]pyrimidine derivatives along with their inhibition properties toward Src in a cell-free assay, as well as their antiproliferative activity toward the A431 and BC-8701 cell lines, was reported, demonstrating that several compounds were more active than PP2, chosen as the reference compound. In detail, the studied compounds were found to block Src phosphorylation, induce apoptosis, and reduce cell proliferation, the activation of Src being an important step in the progression of cancer. Biological data reported here when correlated to the structural properties of the compounds allowed the identification of key elements for the synthesis of new compounds with enhanced capacity to inhibit Src phosphorylation. In fact, an N1 chlorophenyl ethyl side chain in combination with a 6-methylthio group seemed to be the optimal combination of chemical features for antiproliferative activity. On the other hand, substituents at the position 4 of the heterocyclic core appeared to be only responsible for the fine-tuning of the antiproliferative activity. The new compounds may play an important role in the field of anticancer agents, because

they affect a selective pathway that is crucial for the growth of transformed cells. In particular, such compounds showed an important in vitro activity toward 8701-BC cells, suggesting that some of them could be effective agents in the chemotherapy armamentarium against breast cancer (for example, in the multimodality therapies, targeting multiple biological mechanisms)[42,43] and could satisfy the need of new molecules to be used as therapeutical tools for many patients eventually developing resistant cells in the course of their disease.

Experimental Section

Chemistry. Starting materials were purchased from Aldrich-Italia (Milan, Italy). Melting points were determined with a Büchi 530 apparatus and are uncorrected. IR spectra were measured in KBr with a Perkin-Elmer 398 spectrophotometer. ^{1}H NMR spectra were recorded in a $(CD_3)_2SO$ solution on a Varian Gemini 200 (200 MHz) instrument. Chemical shifts are reported as δ (ppm) relative to TMS as internal standard, J in Hz. ^{1}H patterns are described using the following abbreviations: s = singlet, d = doublet, t = triplet, q = quartet, sx = sextect, m = multiplet, br = broad. All compounds were tested for purity by TLC (Merk, Silica gel 60 F_{254}, $CHCl_3$ as eluant). Analyses for C, H, N were within ±0.3% of the theoretical value.

Ethyl 5-{[(Benzoylamino)carbonothioyl]amino}-1-(2-hydroxy-2-phenylethyl)-1*H*-pyrazole-4-carboxylate (9). A suspension of **8** (2.7 g, 10 mmol) and benzoyl isothiocyanate (1.7 g, 11 mmol) in anhydrous tetrahydrofuran (THF) (20 mL) was refluxed for 12 h. The solvent was evaporated under reduced pressure; the oily residue crystallized by adding diethyl ether (30 mL) to afford the pure product **9** (4.07 g, 93%) as a white solid; mp 171−172 °C. ^{1}H NMR: δ 1.29 (t, J = 7.0, 3H, CH_3), 3.97−4.20 (m, 5H, $2CH_2$ + OH, 1H disappears with D_2O), 4.58−4.68 (m, 1H, CHO), 7.05−7.98 (m, 10H Ar), 8.02 (s, 1H, H-3), 8.70 (s, 1H, NH, disappears with D_2O), 12.05 (s, 1H, NH, disappears with D_2O). IR cm^{-1}: 3221 (NH), 3190−2940 (OH), 1708 and 1671 (2 CO). Anal. ($C_{22}H_{22}N_4O_4S$) C, H, N, S.

1-(2-Hydroxy-2-phenylethyl)-6-thioxo-1,5,6,7-tetrahydro-4*H*-pyrazolo[3,4-*d*]pyrimidin-4-one (10). A solution of **9** (4.38 g, 10 mmol) in 2 M NaOH (40 mL) was refluxed for 10 min and successively diluted with H_2O (40 mL). The solution was acidified with glacial acetic acid. After being stored in a refrigerator for 12 h, a solid crystallized and was filtered and recrystallized from absolute ethanol to give **10** (2.3 g, 80%) as a white solid; mp 264−265 °C. ^{1}H NMR: δ 4.15−4.30 and 4.55−4.72 (2m, 2H, CH_2N), 4.85−5.00 (m, 1H, CHO), 5.66 (br s, 1H, OH, disappears with D_2O), 7.20−7.51 (m, 5H Ar), 8.02 (s, 1H, H-3), 12.20 (s, 1H, NH, disappears with D_2O), 13.40 (s, 1H, NH, disappears with D_2O). IR cm^{-1}: 3362 (NH), 3242−2973 (OH), 1681 (CO). Anal. ($C_{13}H_{12}N_4O_2S$) C, H, N, S.

1-(2-Hydroxy-2-phenylethyl)-6-(methylthio)-1,5-dihydro-4*H*-pyrazolo[3,4-*d*]pyrimidin-4-one (11a). A solution of **10** (2.88 g, 10 mmol) and methyl iodide (7.10 g, 50 mmol) in anhydrous THF (20 mL) was refluxed for 12 h. The solvent and the excess of methyl iodide were removed by distillation under reduced pressure; the oily residue crystallized by adding $CHCl_3$ (10 mL) and was purified by recrystallization with absolute ethanol to give **11a** (2.17 g, 72%) as a white solid; mp 208−209 °C. ^{1}H NMR: δ 2.51 (s, 3H, CH_3S), 4.27−4.50 (m, 2H, CH_2N), 5.04−5.18 (m, 1H, CHO), 5.68 (d, 1H, OH, disappears with D_2O), 7.20−7.42 (m, 5H Ar), 7.97 (s, 1H, H-3). IR cm^{-1}: 3544 (NH), 3450−3100 (OH), 1678 (CO). Anal. ($C_{14}H_{14}N_4O_2S$) C, H, N, S.

1-(2-Hydroxy-2-phenylethyl)-6-(ethylthio)-1,5-dihydro-4*H*-pyrazolo[3,4-*d*]pyrimidin-4-one (11b). Compound **11b** was prepared according to the synthetic sequence described for compound **11a**, by using ethyl iodide as alkylating agent. In this case, the crude product was purified by column chromatography (silica gel, 100 mesh) using a mixture of $CHCl_3$:MeOH (9:1) as the eluant, to afford the pure product **11b** (2.05 g, 65%) as a light yellow solid: mp 199−200 °C. ^{1}H NMR: δ 1.45 (t, J = 7.4, 3H, CH_3), 3.22 (q, J = 7.4, 2H, CH_2S), 4.44−4.68 (m, 2H, CH_2N), 5.21−5.30 (m, 1H, CHO), 7.26−7.47 (m, 5H Ar), 8.10 (s, 1H, H-3). IR cm^{-1} 3470 (NH), 3450−3140 (OH), 1670 (CO). Anal. ($C_{15}H_{16}N_4O_2S$) C, H, N, S.

4-Chloro-1-(2-chloro-2-phenylethyl)-6-(methylthio)-1*H*-pyrazolo[3,4-*d*]pyrimidine (12a). The Vilsmeier complex, previously prepared from $POCl_3$ (6.13 g, 40 mmol) and anhydrous dimethylformamide (DMF) (2.92 g, 40 mmol) was added to a suspension of **11a** (3.02 g, 10 mmol) in $CHCl_3$ (20 mL). The mixture was refluxed for 4 h. The solution was washed with H_2O (2 × 20 mL), dried ($MgSO_4$), filtered, and concentrated under reduced pressure. The crude oil was purified by column chromatography (silica gel, 100 mesh), using a mixture of diethyl ether/petroleum ether (bp 40−60 °C) (1:1) as the eluant, to afford the pure product **12a** (2.2 g, 65%) as a white solid, mp 95−96 °C. ^{1}H NMR: δ 2.62 (s, 3H, CH_3S), 4.77−5.05 (m, 2H, CH_2N), 5.45−5.56 (m, 1H, CHCl), 7.29−7.46 (m, 5H Ar), 8.02 (s, 1H, H-3). Anal. ($C_{14}H_{12}N_4SCl_2$) C, H, N, S.

4-Chloro-1-(2-chloro-2-phenylethyl)-6-(ethylthio)-1*H*-pyrazolo[3,4-*d*]pyrimidine (12b). Compound **12b** was prepared according to the synthetic sequence described for compound **12a**, starting from **11b**, to afford the pure product **12b** (2.12 g, 60%) as a white solid, mp 89−90 °C. ^{1}H NMR: δ 1.49 (t, J = 7.2, 3H, CH_3), 3.23 (q, J = 7.2, 2H, CH_2S), 4.75−5.03 (m, 2H, CH_2N), 5.43−5.57 (m, 1H, CHCl), 7.28−7.47 (m, 5H Ar), 8.04 (s, 1H, H-3). Anal. ($C_{15}H_{14}N_4SCl_2$) C, H, N, S.

General Procedure for Compounds 1a−l and 2a−g. To a solution of **12a** or **12b** (10 mmol) in anhydrous toluene (20 mL) was added the appropriate amine (40 mmol), and the reaction mixture was stirred at room temperature for 24 h. The mixture was washed with H_2O (2 × 10 mL), and the organic phase was dried ($MgSO_4$), filtered and evaporated under reduced pressure; the oily residue crystallized by adding petroleum ether (bp 40−60 °C) (10 mL), to give the final products **1a−l** and **2a−g**.

1-(2-Hydroxy-2-phenylethyl)-1,5-dihydro-4*H*-pyrazolo[3,4-*d*]-pyrimidin-4-one (13). A suspension of **8** (2.75 g, 10 mmol) in formamide (10 g, 333 mmol) was heated at 190 °C for 8 h and then poured in H_2O (300 mL). The crude product was filtered and purified by dissolving in 2 M NaOH (100 mL) and boiling with charcoal, followed by precipitation with glacial acetic acid. The solid was filtered and recrystallized from absolute ethanol to give **13** (1.79 g, 70%) as a white solid: mp 270−271 °C. ^{1}H NMR: δ 4.25−4.55 (m, 2H, CH_2), 5.05−5.15 (m, 1H, CHO), 5.65 (d, 1H, OH, disappears with D_2O), 7.25−7.45 (m, 5H Ar), 8.05 (s, 1H, H-3), 8.10 (s, 1H, H-6), 12.15 (br s, 1H, NH, disappears with D_2O). IR cm^{-1}: 3400 (NH), 3245−2900 (OH), 1740 (CO). Anal. ($C_{13}H_{12}N_4O_2$) C, H, N.

4-Chloro-1-(2-phenylvinyl)-1*H*-pyrazolo[3,4-*d*]pyrimidine (14). $POCl_3$ (14 g, 91 mmol) was added to **13** (2.56 g, 10 mmol) and the mixture was refluxed for 12 h and then cooled to room temperature. The excess of $POCl_3$ was removed by distillation under reduced pressure. H_2O (20 mL) was carefully added to the residue, and the suspension was extracted with $CHCl_3$ (3 × 20 mL). The organic solution was washed with H_2O (10 mL), dried ($MgSO_4$), filtered, and concentrated under reduced pressure. The crude brown oil was purified by column chromatography (Florisil 100−200 mesh), using $CHCl_3$ as the eluant to afford the pure product **14** (1.66 g, 65%) as a white solid: mp 139−140 °C. ^{1}H NMR: δ 7.25−7.61 (m, 6H, 5H Ar + CH═), 8.04 (d, J_{trans} = 14.6, 1H, CH═), 8.29 (s, 1H, H-3), 8.85 (s, 1H, H-6). IR cm^{-1}: 1658 (C═C). Anal. ($C_{13}H_9N_4Cl$) C, H, N.

General Procedure for Compounds 5a−k. Compounds **5a−k** were prepared according to the synthetic sequence described for compounds **1** and **2** starting from the intermediate **14**.

2-(4-Bromo-1*H*-pyrazolo[3,4-*d*]pyrimidin-1-yl)-1-phenylethanol (15). To a cold (−20 °C) suspension of **13** (2.56 g, 10 mmol) and NBS (7.12 g, 40 mmol) in dry acetonitrile (20 mL) was added hexamethylphosphorus triamide (HMPT) (6.53 g, 40 mmol) dropwise. After addition, the cold bath was removed and the reaction mixture stirred at room temperature for 0.5 h. LiBr (3.44 g, 40 mmol) was added, and the mixture was heated at 70 °C for 5 h. The mixture was evaporated under reduced pressure. The dark oil

was purified by column chromatography (silica gel, 100 mesh) using $CHCl_3$ as the eluant, to afford the pure product **15** (1.40 g, 44%) as a white solid: mp 146−147 °C. ^{1}H NMR: δ 3.46−3.53 (br s, 1H, OH, disappears with D_2O), 4.57−4.79 (m, 2H, CH_2N), 5.18−5.29 (m, 1H, CHO), 7.30−7.52 (m, 5H Ar), 8.01 (s, 1H, H-3), 8.48 (s, 1H, H-6). IR cm^{-1}: 3240−2500 (OH). Anal. ($C_{13}H_{11}N_4OBr$) C, H, N.

General Procedure for Compounds 6a−g. Compounds **6a−g** were prepared according to the synthetic sequence described for compound **1**, **2** and **5** starting from the intermediate **15**.

General Procedure for Compounds 3a−e and 4a,b. DBU (5 g, 33.44 mmol) was added to **1j, 1k, 1f, 1g, 1l, 2e,** and **2g** (10 mmol). The mixture was heated at 90 °C for 8 h. Absolute ethanol (5 mL) was added to give the crudes (**3a−e** and **4a**,**b**, respectively), which were then recrystallized from absolute ethanol.

1-(2-Bromo-2-phenylethyl)-1,5-dihydro-4*H*-pyrazolo[3,4-*d*]pyrimidin-4-one (16). To a suspension of **13** (2.56 g, 10 mmol), in anhydrous DMF (20 mL), cooled at 0° C, was added a solution of phoshorous tribromide (3.27 g, 12,1 mmol), pyridine (0.5 mL) and toluene (5 mL) previously prepared, dropwise. The mixture was stirred at r.t. for 3 days. The solvent was removed under reduced pressure, and the residue was poured in water and ice (200 mL). The solid was filtered and recrystallized from absolute ethanol, to give the pure product **16** (1.91 g; 60%), as a white solid; mp 230−231 °C. ^{1}H NMR: δ 4.80−4.97 and 5.01−5.19 (2m, 2H, CH_2N), 5.68−5.72 (m, 1H, CHBr), 7.30−7.65 (m, 5H Ar), 7.97 (s, 1H, H-3), 8.13 (s, 1H, H-6), 12.25 (br s, 1H, NH, disappears with D_2O). IR cm^{-1}: 3440 (NH), 1665 (C═O). Anal. ($C_{13}H_{11}N_4BrO$) C, H, N.

1-(2-Bromo-2-phenylethyl)-4-chloro-1*H*-pyrazolo[3,4-*d*]pyrimidine (17). The Vilsmeier complex, previously prepared from $POCl_3$ (15.3 g, 100 mmol) and anhydrous dimethylformamide (DMF) (7.3 g, 100 mmol) was added to a suspension of **16** (3.19 g, 10 mmol) in $CHCl_3$ (50 mL). The mixture was refluxed for 12 h. The solution was washed with H_2O (2 × 20 mL), dried ($MgSO_4$), filtered, and concentrated under reduced pressure. The crude oil was purified by column chromatography (Florisil, 100 mesh), using Et_2O as eluant, to afford the pure product **17** (2.63 g, 78%) as a white solid, mp 114−115 °C. ^{1}H NMR: δ 4.95−5.10 and 5.18−5.38 (2m, 2H, CH_2N), 5.58−5.78 (m, 1H, CHBr), 7.25−7.70 (m, 5H Ar), 8.17 (s, 1H, H-3), 8.77 (s, 1H, H-6). Anal. ($C_{13}H_{10}N_4BrCl$) C, H, N.

General Procedure for the 4-Amino-Substituted 1-(2-Bromo-2-phenylethyl)-1*H*-pyrazolo[3,4-*d*]pyrimidines (7a−k). To a solution of **17** (1.69 g, 5 mmol) in anhydrous toluene (20 mL) was added the proper amine (20 mmol), and the reaction mixture was stirred at room temperature for 36 h. After it was extracted with H_2O (2 × 20 mL), the organic phase was dried ($MgSO_4$), filtered, and concentrated under reduced pressure; the oily residue crystallized by adding Et_2O (10 mL) to give products **7a−k**.

Biology. Enzymatic Assay. Recombinant human Src was purchased from Upstate (Lake Placid, NY). Activity was measured in a filter-binding assay using a commercial kit (Src Assay Kit, Upstate), according to the manufacturer's protocol, using 150 μM of the specific Src peptide substrate (KVEKIGEGTYGVVYK) and in the presence of 0.125 pmol of Src and 0.160 pmol of [γ-^{32}P]-ATP. The apparent affinity (K_m) values of the Src preparation used for its peptide and ATP substrates were determined separately and found to be 30 μM and 5 μM, respectively.

Kinetic Analysis. Dose−response curves where generated by fitting the data by computer simulation to eq 1: $E_{(\%)} = E_{max}/(1 + [I]/ID_{50})$, where $E_{(\%)}$ is the fraction of the enzyme activity measured in the presence of the inhibitor, E_{max} is the activity in the absence of the inhibitor, [I] is the inhibitor concentration, and ID_{50} is the inhibitor concentration at which $E_{(\%)} = 0.5E_{max}$.

The ID_{50} were converted to K_i according to a competitive mechanism with respect to the substrate ATP. The second substrate of the reaction (the peptide) was kept at saturating concentrations (4-fold higher its K_m). Since (i) the ATP concentration was limiting, i.e., [ATP] $\ll K_{m(ATP)}$, and (ii) the enzyme concentration was not negligible with respect to the ATP concentration, i.e., [E] $\geq$ [ATP], the classical Cheng−Prusoff relationship was not applicable. Instead, K_i values were calculated according to eq 2: $K_i = (ID_{50} - E_0/2)/\{E_0 - [S_0/K_m - 1]/E_0\}$, where S_0 is the concentration of the competing substrate (ATP), and E_0 is the concentration of the enzyme. Each experiment was in triplicate and mean values were used for the interpolation. Curve fitting was performed with the program GraphPad Prism.

Cell Culture. Human epidermoid carcinoma A431 cells[44] were obtained from the American Type Culture Collection and were grown in Dulbecco's modified Eagle's medium containing 10% fetal calf serum. The highly metastatic 8701-BC breast cancer cell line[45] (kindly provided by Prof. I. Pucci-Minafra, University of Palermo, Italy) was maintained as monolayer cultures in RPMI 1640 medium (BioWhittaker, Vallensbaek, DK) containing 10% fetal calf serum. 8701-BC cell line deserves particular attention, since it was established from a primary DIC, that is, before the clonal selection of the metastatic process. This cell line maintains a number of properties in culture that are typical of the mammary tumor cells and is known to overexpress Src tyrosine kinase.[21] The cultures were free of Mycoplasma. For proliferation assay cells line (2×10^4 cells/mL) were incubated in 100 μL of RPMI 1640 culture medium (BioWhittaker, Vallensbaek, DK), supplemented with 10% fetal calf serum (FCS; BioWhittaker, Vallensbaek, DK) and antibiotics (100 U/mL penicillin and 100 μg/mL streptomycin), at 37 °C in 5% CO_2 for 8 h, to allow adhesion. After adhesion, the medium was replaced with 100 μL of medium supplemented with 0.5% FCS. After an overnight incubation, the spent medium was then removed, and the cultures were refreshed with new medium (100 μL of RPMI 1640 with 10% FCS) or medium along with different concentrations (0−100 μM) of the studied compounds. After 3 days (control cultures did not reach confluence), the antiproliferative effect of the compounds was determined by 3-(4,5-dimethylthiazol-2-yl)-2,5-diphenyl-tetrazolium bromide (MTT) proliferation assay.[46] Briefly, cells were treated with 10 μL of the MTT solution (5 mg/mL). Four h later, 100 μL of acid propan-2-ol (0.04 M HCl in propan-2-ol) were added to dissolve the formazan product. The microplates were read using an ELISA plate reader at 570 nm with a reference wavelength of 630 nm. Data analysis for IC_{50} calculations was performed with the LSW Data Analysis Package plug-in for Excel (Microsoft). Result are reported as mean ± SEM of five experiments performed in triplicate.

Western Blot. The inhibitory effects of compounds toward the phosphorylation of Src (Tyr419) were evaluated using immunoblot analyses. Cell lines were cultured at a concentration of 2×10^4 cells/mL, challenged with the compounds (10 μM) for 3 h, and then treated with 100 nM EGF (Cell Signaling Technology). Five minutes later, cells were harvested and lysed in an appropriate buffer containing 1% Triton X-100. Proteins were quantitated by the BCA method (Pierce, Rockford, IL). Equal amounts of total cellular protein were resolved by SDS-polyacrylamide gel electrophoresis, transferred to nitrocellulose filters, and subjected to immunoblot using phospho-specific antibodies against Src (Y419) (Cell Signaling Technology). Filters were additionally reprobed with specific non phospho anti-Src antibodies (Cell Signaling Technology) after stripping. Quantification of phospho and non phospho Src expression was achieved with Sigma Gel analysis software, and results represented the percent of the phospho Scr over non phospho Src. The means ± SEM of three independent experiments are presented. A double asterisk (**) in the right portion of Figures 1, 2, 4, and 5 indicates a significant ($p < 0.05$) effect of EGF treatment (control vs control + EGF). Single asterisks indicate statistically significant differences between control + EGF and cell lines treated with specific compound + EGF. Statistical analyses were performed using Student's *t* test and the Bonferroni's correction. The proapoptotic activity of some of the compounds was also tested, using a Poly-ADP−Ribose-Polymerase (PARP) assay (Roche Diagnostics, Milano, Italy). Cell lines were cultured at a concentration of 2×10^4 cells/mL and challenged with the compounds (10 μM). Three hours later, cells were harvested and lysed as reported above. Immunoblot analysis was performed using PARP-specific antibodies to both the uncleaved (113 kDa) and cleaved (89 kDa) form of

Table 2.

outlev 1	diagnostic output level
rmstol 1.5	cluster_tolerance/A
extnrg 1000.0	external grid energy
e0max 0.0 10000	max initial ernergy; max number of retries
ga_pop_size 200	number of individuals in population
ga_num_evals 1500000	maximum number of energy evaluations
ga_num_generations 50000	maximum number of generations
ga_elitism 1	number of top individuals to survive to next generation
ga_mutation_rate 0.02	rate of gene mutation
ga_crossover_rate 0.8	rate of crossover
ga_window_size 10	
ga_cauchy_alpha 0.0	Alpha parameter of Cauchy distribution
ga_cauchy_beta 1.0	Beta parameter Cauchy distribution
set_ga	set the above parameters for GA or LGA
sw_max_its 300	iterations of Solis & Wets local search
sw_max_succ 4	consecutive successes before changing rho
sw_max_fail 4	consecutive failures before changing rho
sw_rho 1.0	size of local search space to sample
sw_lb_rho 0.01	lower bound on rho
ls_search_freq 0.06	probability of performing local search on individual
set_psw1	set the above pseudo-Solis & Wets parameters
ga_run 250	do this many hybrid GA-LS runs
analysis	perform a ranked cluster analysis

PARP. Quantification of PARP expression was achieved with Sigma Gel analysis software, and the results, representing the percent of cleaved over uncleaved PARP, are expressed as means ± SEM of three independent experiments. Asterisks indicate statistically significant differences ($p < 0.05$) between control and cells lines treated with the tested compound. Statistical analyses were performed using Student's *t* test and the Bonferroni's correction.

Ribonuclease Protection Assay (RPA). The mRNA expression of cyclins and BCL2 gene were performed using RPA. mRNA expression was determined using panels of commercially available probes (Multiprobe Ribonuclease Protection Assay, Pharmingen, San Diego, CA) as previously described.[47] 8701-BC were treated as reported above, but the cells were challenged with the compounds (10 μM) for 3 h for cyclins expression and for 72 h for BCL2 gene expression. Next, the cells were harvested and lysed in an appropriate buffer (OMNIzol for RNA-DNA-Protein Extraction Kit, Euroclone, Devon, UK). The extracts were processed for the extraction of mRNA. The RNA probes were synthesized according to the suggested procedure (MAXIscript, Ambion, Austin, TX), using T7 phage polymerase and a biotin RNA labeling mixture (Boehringer, Mannheim, Germany). Briefly, an equal amount of mRNA extracted from the cell lysates and appropriate RNA probes were hybridized, according to the suggested procedure (Direct Protect, Lysate Ribonuclease Protection Assay Kit, Ambion). The products of RNase protection assay were then separated for analysis on a denaturing polyacrylamide gel (5% acrylamide/8 M urea) by running the gel at 200 V for 1 h. Gels were then transferred to a positively charged nylon membrane, using a semidry transfer unit at 90 mA for 1 h (Hoefer Pharmacia Biotech, San Francisco, CA). The transcripts were then immobilized by UV cross-linking (biolink, Euroclone). Nonisotopic detection was performed with the BrightStar BioDetect kit (Ambion), following the manufacturer's instructions. The identity and quantity of each mRNA species in the original sample was then determined from the signal intensities given by the appropriately sized protected probe fragment bands. Antisense GAPDH and L32 (housekeeping genes) probe transcripts were synthesized and used in a series of parallel reactions, to normalize the amounts of RNA present in the lysates (protected nucleotide size for L32: 112 nt). Gel electrophoretic autoradiographs were then quantitated by Sigma Gel analysis software (Jandel Scientific, San Rafael, CA).

Computational Details. All calculations and graphical manipulations were performed on Silicon Graphics computers (Origin 300 server and Octane workstations) using the software packages Autodock 3.0.5[37] and MacroModel 8.5.[40] Structures of inhibitors were represented using MacroModel and minimized with the Amber force field using the Polak−Ribiere conjugated gradient method (0.001 kJ/mol·Å convergence or 10 000 iterations). To be exported to Autodock, the minimized structures were converted into the mol2 file format using Babel software. Molecular docking and dynamics calculations were performed with MacroModel software.

To remove unfavorable contacts, a preliminary structure optimization was performed on the X-ray crystallographic structure of the active conformation of c-Src (entry 1y57 of the Brookhaven Protein Data Bank, 1.9 Å resolution)[36] through the all-atom Amber* force field and Polak−Ribiere conjugate gradient method. A continuum solvation method, with water as the solvent, was also applied. Extended cutoffs were used and convergence was set to 0.01 kJ/mol·Å. The output structure of Src was imported in Autodock Tools and prepared for docking simulations. To prepare the input structures for Autodock calculations, the Src structure was further manipulated by removing nonpolar hydrogens, while Kollman united-atom partial charges and solvent parameters were added. Similarly to the protein, the structure of the inhibitors was also prepared by deleting their nonpolar hydrogen atoms and adding Gasteiger atomic charges. Finally, the rigid root and rotatable bonds were defined using AutoDockTools.

During the next step, several atom probes (characterized by the same stereoelectronic properties as the atoms constituting the inhibitor) were moved on the grid nodes, while the interaction energy between the probe and the inhibitor was calculated at each node. In such a way, grid maps can be generated for each atom probe, describing its interactions with the inhibitor. Autogrid 3.0, as implemented in the Autodock 3.0 software package, was used to generate grid maps. The Lamarckian genetic algorithm (LGA)[37] was employed to generate orientations/conformations of the ligand within the binding site. Parameters for blind docking runs are shown in Table 2 (imported from a docking parameter file), on the basis of literature suggestions.[48]The choice of the best conformation was based on the assumption that, although for high throughput screening protocols, only the first ranked conformation should be considered (that is, the conformation characterized by the lowest estimated free energy of binding);[49] in other cases, the lowest energy conformation of the most populated cluster should be also taken into account.[50]

The reliability of the docking protocol was first tested by simulations of the binding mode of PP2, and comparison of the modeled complex with the available three-dimensional structure derived by X-ray crystallography of the complex between PP2 and Lck. The program successfully reproduced the X-ray coordinates of the inhibitor binding conformation, as well as the features of pharmacophoric models reported in the literature.[38]

Acknowledgment. Financial support provided by the Italian MIUR (Cofin 2004-prot. 2004059221_004) and by the Fondazi-

one Monte dei Paschi di Siena is gratefully acknowledged. We thank Dr. Giovanni Gaviraghi (Sienabiotech S.p.A.) for helpful discussion. The "Centro Universitario per l'Informatica e la Telematica" of the University of Siena is also acknowledged.

Supporting Information Available: Experimental details of the synthesis, spectral data, and elemental analysis data of some representative compounds. This material is available free of charge via the Internet at http://pubs.acs.org.

References

(1) Neet, K.; Hunter, T. Vertebrate nonreceptor protein-tyrosine kinase families. *Genes Cells* **1996**, *1*, 147−169.

(2) Hunter, T. The role of tyrosine phosphorylation in cell growth and disease. *Harvey Lect.* **1998**, *94*, 81−119.

(3) Ullrich, A.; Schlessinger, J. Signal transduction by receptors with tyrosine kinase activity. *Cell* **1990**, *61*, 203-212.

(4) van der Geer, P.; Hunter, T.; Lindberg, R. A. Receptor protein-tyrosine kinases and their signal transduction pathways. *Annu. Rev. Cell Biol.* **1994**, *10*, 251−337.

(5) Brown, M. T.; Cooper, J. A. Regulation, substrates and functions of src. *Biochim. Biophys. Acta* **1996**, *1287*, 121−149.

(6) Thomas, S. M.; Brugge, J. S. Cellular functions regulated by Src family kinases. *Annu. Rev. Cell Dev. Biol*. **1997**, *13*, 513−609.

(7) Abram, C. L.; Courtneidge, S. A. Src family tyrosine kinases and growth factor signaling. *Exp. Cell Res*. **2000**, *254*, 1−13.

(8) Martin, G. S. The hunting of the Src. *Nat. Rev. Mol. Cell Biol.* **2001**, *2*, 467−475.

(9) Frame, M. C.; Fincham, V. J.; Carragher, N. O.; Wyke, J. A. v-Src's hold over actin and cell adhesions. *Nat. Rev. Mol. Cell Biol.* **2002**, *3*, 233−245.

(10) Bjorge, J. D.; Jakymiw, A.; Fujita, D. J. Selected glimpses into the activation and function of Src kinase. *Oncogene* **2000**, *19*, 5620−5635.

(11) Mazurenko, N. N.; Kogan, E. A.; Zborovskaya, I. B.; Kisseljov, F. L. Expression of pp60c-src in human small cell and non small cell lung carcinomas. *Eur. J. Cancer* **1992**, *28*, 372−377.

(12) Irby, R. B.; Yeatman, T. J. Role of Src expression and activation in human cancer. *Oncogene* **2000**, *19*, 5636−5642.

(13) Budde, R. J.; Ke, S.; Levin, V. A. Activity of pp60c-src in 60 different cell lines derived from human tumors. *Cancer Biochem. Biophys.* **1994**, *14*, 171−175.

(14) Irby, R. B.; Mao, W.; Coppola, D.; Kang, J.; Loubeau, J. M.; Trudeau, W.; Karl, R.; Fujita, D. J.; Jove, R.; Yeatman, T. J. Activating SRC mutation in a subset of advanced human colon cancers. *Nat. Genet.* **1999**, *21*, 187−190.

(15) Verbeek, B. S.; Vroom, T. M.; Adriaansen-Slot, S. S.; Ottenhoff-Kalff, A. E.; Geertzema, J. G.; Hennipman, A.; Rijksen, G. c-Src protein expression is increased in human breast cancer. An immunohistochemical and biochemical analysis. *J. Pathol.* **1996**, *180*, 383−388.

(16) Barrios Sosa, A. C.; Boschelli, D. H.; Wu, B.; Wang, Y.; Golas, J. M. Further studies on ethenyl and ethynyl-4-phenylamino-3-quinolinecarbonitriles: identification of a subnanomolar Src kinase inhibitor. *Bioorg. Med. Chem. Lett.* **2005**, *15*, 1743−1747.

(17) Plé, P. A.; Green, T. P.; Hennequin, L. F.; Curwen, J.; Fennel, M.; Allen, J.; Lambert-van der Brempt, C.; Costello, G. Discovery of a new class of anilinoquinazoline inhibitors with high affinity and specificity for the tyrosine kinase domain of c-Src. *J. Med. Chem.* **2004**, *47*, 871−887.

(18) Altmann, E.; Widler, L.; Missbach, M. *N*(7)-substituted-5-aryl-pyrrolo[2,3-*d*]pyrimidines represent a versatile class of potent inhibitors of the tyrosine kinase c-Src. *Mini Rev. Med. Chem.* **2002**, *2*, 201−208.

(19) Hanke, J. H.; Gardner, J. P.; Dow, R. L.; Changelian, P. S.; Brissette, W. H.; Weringer, E. J.; Pollok, B. A.; Connelly, P. A. Discovery of a novel, potent, and Src family-selective tyrosine kinase inhibitor. Study of Lck- and FynT-dependent T cell activation. *J. Biol. Chem.* **1996**, *271*, 695−701.

(20) Schenone, S.; Bruno, O.; Ranise, A.; Bondavalli, F.; Brullo, C.; Fossa, P.; Mosti, L.; Menozzi, G.; Carraro, F.; Naldini, A.; Bernini, C.; Manetti, F.; Botta M. New Pyrazolo[3,4-*d*]pyrimidines Endowed with A431 Antiproliferative Activity and Inhibitory Properties of Src Phosphorylation. *Bioorg. Med. Chem. Lett.* **2004**, *14*, 2511−2517.

(21) Sheffield, L. G. C−Src activation by ErbB2 leads to attachment-independent growth of human breast epithelial cells. *Biochem. Biophys. Res. Commun.* **1998**, *250*, 27−31.

(22) It is well-known that breast cancer has been the most common malignancy among western women and the incidence rates of first primary breast cancer have been increasing over time (Chen, Y.; Thompson, W.; Semenciw, R.; Mao, Y. Epidemiology of controlateral breast cancer. *Epidemiol. Biomarkers Prev.* **1999**, *8*, 855−861). Among this tumor type, ductal infiltrating carcinoma (DIC) of the breast is the most common and potentially aggressive form of cancer (Donegan, W. L. Tumor-related prognostic factors for breast cancer. *CA Cancer J. Clin.* **1997**, *47*, 28−51), for the treatment of which there is no approved drug, yet.

(23) Carraro, F.; Pucci, A.; Naldini, A.; Schenone, S.; Bruno, O.; Ranise, A.; Bondavalli, F.; Brullo, C.; Fossa, P.; Menozzi, M.; Mosti, L.; Manetti, F.; Botta, M. Pyrazolo[3,4-*d*]pyrimidines Endowed with Antiproliferative Activity on Ductal Infiltrating Carcinoma Cells. *J. Med. Chem.* **2004**, *47*, 1595−1598.

(24) Bondavalli, F.; Botta, M.; Bruno, O.; Ciacci, A.; Corelli, F.; Fossa, P.; Lucacchini, A.; Manetti, F.; Martini, C.; Menozzi, G.; Mosti, L.; Ranise, A.; Schenone, S.; Tafi, A.; Trincavelli, M. L. Synthesis, molecular modeling studies, and pharmacological activity of selective A_1 receptor antagonists. *J. Med. Chem.* **2002**, *45*, 4875−4887.

(25) Véliz, E. A.; Beal, P. A. C6 substitution of inosine using hexamethylphosphorous triamide in conjunction with carbon tetrahalide or N-halosuccinimide. *Tetrahedron Lett.* **1999**, *41*, 1695−1697.

(26) Liu, Y.; Bishop, A.; Witucki, L.; Kraybill, B.; Shimizu, E.; Tsien, J.; Ubersax, J.; Blethrow, J.; Morgan, D. O.; Shokat, K. M. Structural basis for selective inhibition of Src family kinases by PP1. *Chem. Biol.* **1999**, *6*, 671−678.

(27) Thomas, S. M.; Brugge, J. S. Cellular functions regulated by Src family kinases. *Annu. Rev. Cell Dev. Biol.* **1997**, *13*, 513−609.

(28) Maga, G. Manuscript in preparation.

(29) Dehm, S. M.; Bonham, K. SRC gene expression in human cancer: the role of transcriptional activation. *Biochem. Cell. Biol.* **2004**, *82*, 263−74.

(30) Botta, M. Manuscript in preparation.

(31) Stout, T. J.; Foster, P. G.; Matthews, D. J. High-Throughput Structural Biology in Drug Discovery: Protein Kinases. *Curr. Pharm. Des.* **2004**, *10*, 1069−1082.

(32) Noble, M. E.; Endicott, J. A.; Brown, N. R.; Johnson, L. N. The cyclin box fold: protein recognition in cell-cycle and transcription control. *Trends Biochem. Sci.* **1997**, *22*, 482−487.

(33) De Murcia, G.; Menissier, D. M. Poly(ADP-ribose) polymerase: a molecular nick-sensor. *Trends Biochem. Sci.* **1994**, *19*, 172−176.

(34) Tewari, M.; Quan, L. T.; O'Rourke, K.; Desnoyers, S.; Zeng, Z.; Beidler, D. R.; Poirier, G. G.; Salvesen, G. S.; Dixit, V. M. Yama/CPP32 beta, a mammalian homolog of CED-3, is a CrmA-inhibitable protease that cleaves the death substrate poly(ADP-ribose) polymerase. *Cell* **1995**, *81*, 801−809.

(35) Cory, S. Regulation of lymphocyte survival by the bcl-2 gene family. *Annu. Rev. Immunol.* **1995**, *13*, 513−543.

(36) Cowan-Jacob, S. W.; Fendrich, G.; Manley, P. W.; Jahnke, W.; Fabbro, D.; Liebetanz, J.; Meyer, T. The Crystal Structure of a C-Src Complex in an Active Conformation Suggests Possible Steps in C−Src Activation. *Structure* **2005**, *13*, 861−871.

(37) Morris, G. M.; Goodsell, D. S.; Halliday, R. S.; Huey, R.; Hart, W. E.; Belew, R. K.; Olson, A. J. Automated Docking Using a Lamarckian Genetic Algorithm and Empirical Binding Free Energy Function. *J. Comput. Chem.* **1998**, *19*, 1639−1662.

(38) Traxler, P.; Bold, G.; Frei, J.; Lang, M.; Lydon, N.; Mett, H.; Buchdunger, E.; Meyer, T.; Mueller, M.; Furet, P. Use of a pharmacophore model for the design of EGF−R tyrosine kinase inhibitors: 4-(phenylamino)pyrazolo[3,4-*d*]pyrimidines. *J. Med. Chem.* **1997**, *40*, 3601−16.

(39) Zhu, X.; Kim, J. L.; Newcomb, J. R.; Rose, P. E.; Stover, D. R.; Toledo, L. M.; Zhao, H.; Morgenstern, K. A. Structural analysis of the lymphocyte-specific kinase Lck in complex with non-selective and Src family selective kinase inhibitors. *Structure Fold. Des.* **1999**, *7*, 651−61.

(40) MacroModel version 8.5. 2003. Schrodinger, L.L.C.

(41) Cona, A.; Manetti, F.; Leone, R.; Corelli, F.; Tavladoraki, P.; Polticelli, F.; Botta, M.Molecular Basis for the Binding of Competitive Inhibitors of Maize Polyamine Oxidase. *Biochemistry* **2004**, *43*, 3426−3435.

(42) Fidler, I. J. The organ microenvironment and cancer metastasis. *Differentiation* **2002**, *70*, 498−505.

(43) Fidler, I. J. The pathogenesis of cancer metastasis: the 'seed and soil' hypothesis revisited. *Nat. Rev. Cancer* **2003**, *3*, 453−458.

(44) Giard, D. J.; Aaronson, S. A.; Todaro, G. J.; Arnstein, P.; Kersey, J. H.; Dosik, H.; Parks, W. P. In vitro cultivation of human tumors: establishment of cell lines derived from a series of solid tumors. *J. Natl. Cancer Inst.* **1973**, *51*, 1417−1423.

(45) Minafra, S.; Morello, V.; Glorioso, F.; La Fiura, A. M.; Tomasino, R. M.; Feo, S.; McIntosh, D.; Woolley, D. E. A new cell line (8701-BC) from primary ductal infiltrating carcinoma of human breast. *Br. J. Cancer* **1989**, *60*, 185−192.

(46) Mosmann, T. Rapid colorimetric assay for cellular growth and survival: application to proliferation and cytotoxicity assays. *J. Immunol. Methods* **1983**, *65*, 55−63.

(47) Naldini, A.; Carraro, F. Hypoxia modulates cyclin and cytokine expression and inhibits peripheral mononuclear cell proliferation. *J. Cell. Physiol.* **1999**, *181*, 448−454.
(48) Hetenyi, C.; van der Spoel, D. Efficient docking of peptides to proteins without prior knowledge of the binding site. *Prot. Sci.* **2002**, *11*, 1729−1737.
(49) Ren, J.; Esnouf, R.; Garman, E.; Somers, D.; Ross, C.; Kirby, I.; Keeling, J.; Darby, G.; Jones, Y.; Stuart, D. High-resolution structures of HIV-1 RT from four RT-inhibitor complexes. *Nat. Struct. Biol.* **1995**, *2*, 293−302.
(50) Ragno, R.; Mai, A.; Massa, S.; Cerbara, I.; Valente, S.; Bottoni, P.; Scatena, R.; Jesacher, F.; Loidl, P.; Brosch, G. 3-(4-Aroyl-1-methyl-1*H*-pyrrol-2-yl)-*N*-hydroxy-2-propenamides as a New Class of Synthetic Histone Deacetylase Inhibitors. 3. Discovery of Novel Lead Compounds through Structure-Based Drug Design and Docking Studies. *J. Med. Chem.* **2004**, *47*, 1351−1359.

JM050603R